Rapid in vitro prototyping of O-methyltransferases for pathway applications in Escherichia coli

Haslinger, Kristina; Hackl, Thomas; Prather, Kristala L J

Published in:
Cell Chemical Biology

DOI:
10.1016/j.chembiol.2021.04.010

Publication date:
2021

Cell Chemical Biology

Rapid *in vitro* prototyping of *O*-methyltransferases for pathway applications in *Escherichia coli*

Graphical abstract

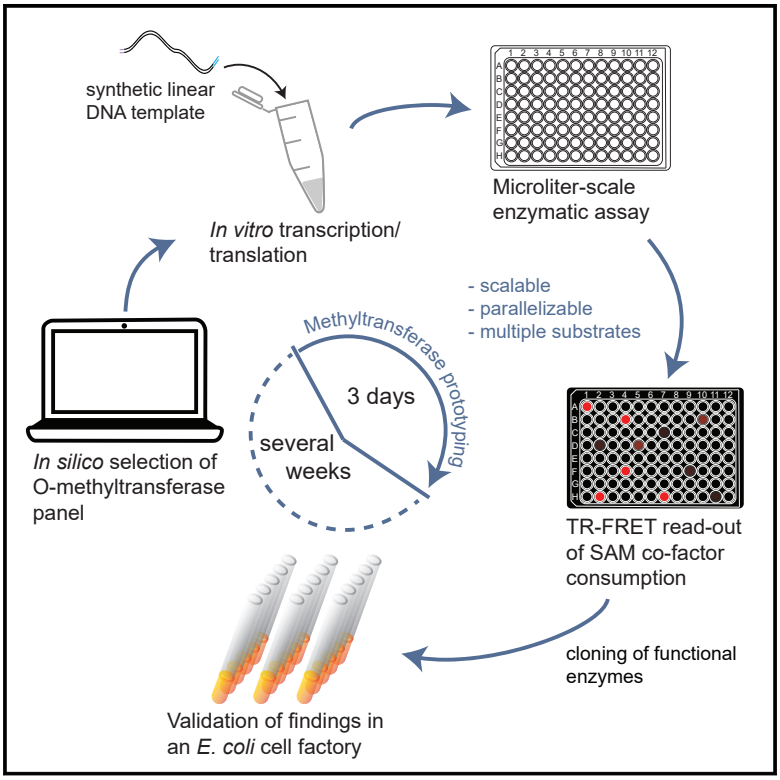

Highlights

- We developed a time- and resource-saving qualitative screen for OMTs
- TXTL from linear templates eliminated time-consuming cloning
- Small-scale enzymatic assays were compatible with the crude TXTL reactions
- FRET-based readout allowed parallelized analysis of 180 assay reactions in 3 h

Authors

Kristina Haslinger, Thomas Hackl, Kristala L.J. Prather

Correspondence

k.haslinger@rug.nl (K.H.), kljp@mit.edu (K.L.J.P.)

In brief

Methylation is an important reaction in medicinal chemistry that can be carried out by enzymes under mild conditions. Identifying the appropriate methyltransferase, however, is a resource-consuming process. Haslinger et al. developed a rapid prototyping workflow for *O*-methyltransferases that should be applicable to all *S*-adenosylmethionine-dependent methyltransferases.

Haslinger et al., 2021, Cell Chemical Biology *28*, 876–886
June 17, 2021
https://doi.org/10.1016/j.chembiol.2021.04.010

CellPress

CellPress

Cell Chemical Biology

Resource

Rapid *in vitro* prototyping of *O*-methyltransferases for pathway applications in *Escherichia coli*

Kristina Haslinger,[1,2,*] Thomas Hackl,[3] and Kristala L.J. Prather[1,4,*]

[1]Department of Chemical Engineering, Massachusetts Institute of Technology, Cambridge, MA 02139, USA

[2]Department of Chemical and Pharmaceutical Biology, University of Groningen, 9713 AV Groningen, The Netherlands

[3]Biomolecular Mechanisms, Max Planck Institute for Medical Research, 69121 Heidelberg, Germany

[4]Lead contact

*Correspondence: k.haslinger@rug.nl (K.H.), kljp@mit.edu (K.L.J.P.)

https://doi.org/10.1016/j.chembiol.2021.04.010

SUMMARY

O-Methyltransferases are ubiquitous enzymes involved in biosynthetic pathways for secondary metabolites such as bacterial antibiotics, human catecholamine neurotransmitters, and plant phenylpropanoids. While thousands of putative *O*-methyltransferases are found in sequence databases, few examples are functionally characterized. From a pathway engineering perspective, however, it is crucial to know the substrate and product ranges of the respective enzymes to fully exploit their catalytic power. In this study, we developed an *in vitro* prototyping workflow that allowed us to screen ~30 enzymes against five substrates in 3 days with high reproducibility. We combined *in vitro* transcription/translation of the genes of interest with a microliter-scale enzymatic assay in 96-well plates. The substrate conversion was indirectly measured by quantifying the consumption of the *S*-adenosyl-L-methionine co-factor by time-resolved fluorescence resonance energy transfer rather than time-consuming product analysis by chromatography. This workflow allowed us to rapidly prototype thus far uncharacterized *O*-methyltransferases for future use as biocatalysts.

INTRODUCTION

Methylation of secondary metabolites is a prevalent reaction that alters the bioavailability and reactivity of molecules (Liscombe et al., 2012). This effect is important for the native function of secondary metabolites for the producer organism but also for pharmaceutical and nutraceutical applications of natural products. One example is the oxygen-directed methylation (*O*-methylation) of the lignin precursor caffeic acid toward ferulic acid. This reaction is crucial for regulating the rigidity of lignified cell walls in vascular plants (Vanholme et al., 2010) and has been described to modulate the cytotoxicity and radical scavenging properties of isolated phenolic acids when tested for pharmaceutical applications such as neuroprotection (Kadoma and Fujisawa, 2008; Taram et al., 2016). Similar observations were made for methylated flavonoids (plants) (Koirala et al., 2016; Wen et al., 2017), antimicrobial peptides (bacteria) (Li et al., 2013; Das et al., 2017), and dopamine (humans) (Zahid Khan and Nawaz, 2016). *O*-Methylation in nature is carried out by methyltransferases under the utilization of *S*-adenosyl-L-methionine (SAM; see schematic in Figure S1) as an electron-deficient methyl donor, thereby forming *S*-adenosyl-L-homocysteine (SAH). Some *O*-methyltransferase (OMT) families additionally require the presence of metal ions such as Mg^{2+}. For OMTs acting on small molecules (excluding nucleic acids and proteins), there are several protein families with distinct sequence motifs and a remarkable breadth in functionality. The functional exploration of these families has been somewhat anecdotal to date and has been very much focused on plant enzymes of the methyltransferase families 2 (Pfam: PF00891) and 3 (Pfam: PF01596) (Liscombe et al., 2012). This can most likely be attributed to the fact that in the pre-genomic era these plant enzymes already had been studied with biochemical methods (Finkle and Nelson, 1963; Higuchi et al., 1977). However, with the rapid expansion of genomes sequenced to date, the methyltransferase protein families are growing by the minute and functional studies are lagging behind (Hicks and Prather, 2014).

In the last decade rapid advances in parallelization of molecular cloning, enzymatic assays, and even fermentation through liquid handling technologies and automation have greatly increased the throughput of functional studies of enzyme libraries (Chao et al., 2017; Casini et al., 2018). Next to general difficulties in enzyme expression and purification, the bottlenecks in these screening pipelines remain the failing of molecular cloning steps and the throughput of the reaction readout in the absence of colorimetric or fluorometric assays, which requires time-consuming chromatography methods to analyze the products (Jacques et al., 2017; Longwell et al., 2017). To overcome these latter hurdles in the functional screening of

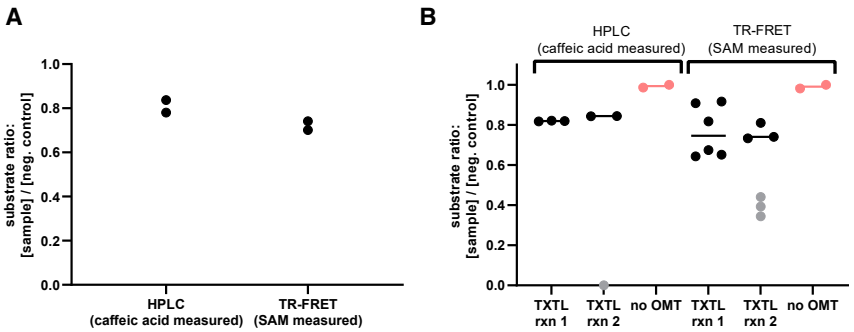

Figure 1. Benchmarking of the OMT screening workflow with the known OMT MxSafC

Substrate detection at the end of the OMT reaction with MxSafC as a catalyst relative to the negative controls measured by HPLC (caffeic acid concentration measured; c_0[caffeic acid] = 2 mM) and TR-FRET (SAM concentration measured; c_0[SAM] = 2 mM).

(A) OMT reaction performed with recombinantly expressed and purified MxSafC (c[MxSafC] = 0.1 mg/mL); data points are biological replicates (n = 2)).

(B) OMT reaction performed with MxSafC expressed from linear DNA in the myTXTL *in vitro* transcription/translation kit. Two biological replicates are shown in separate columns; data points within each column are technical replicates of the OMT reaction and the TR-FRET assay; "no OMT" data points are biological replicates; outliers (gray data points) are likely caused by a pipetting error in the OMT assay and were excluded from determining the median.

See also Figure S2 for representative HPLC chromatograms and calibration curves.

SAM-dependent methyltransferases, we developed a rapid *in vitro* prototyping workflow to express and functionally screen a range of OMTs against several substrates. To minimize time and effort spent on molecular cloning, we employed a recently developed *in vitro* transcription/translation platform for linear DNA templates with high enzyme yields (myTXTL) (Shin and Noireaux, 2010; Garamella et al., 2016) and combined it with a fluorescence-based readout (Heyduk and Heyduk, 2002; Tian et al., 2012) to monitor the consumption of the SAM co-factor. For one substrate, we translated the newly gained knowledge into the development of a microbial cell factory to produce ferulic acid from simple building blocks.

RESULTS

Design and benchmarking of the prototyping workflow

To facilitate the fast screening of a library of putative OMTs against several substrates, we set out to develop a prototyping method that is rapid and parallelizable. In this context we identified the detection of enzymatic activity and the cloning and expression of the genes of interest as the two major bottlenecks. For the detection of enzymatic activity, we deemed a desirable approach to be independent of the substrates and products and to not require time-consuming chromatography. We turned toward commercially available assays to detect the consumption of the SAM cofactor and decided to use the TR-FRET Bridge-It SAM Fluorescence Assay Kit from Mediomics (St. Louis, MO). In this endpoint assay, SAM binds to a DNA-binding protein and induces the association of two fluorescently labeled DNA fragments (donor and acceptor) for Förster resonance energy transfer (FRET) to occur. To minimize background, we decided to use the "TR" (time-resolved) version of the kit with a lanthanide acceptor fluorophore, whose emission can be detected after a short delay to eliminate scatter and background fluorescence from the donor fluorophore. We hypothesized that in this way, several enzymes could be screened against multiple substrates in parallel in the plate reader, with lower TR-FRET readings observed for active enzyme-substrate combinations. We set out to test this detection method with recombinantly expressed and purified MxSafC, an enzyme known to catalyze the methylation of caffeic acid (Nelson et al., 2007; Siegrist et al., 2017), and to compare the TR-FRET readout with product analysis by high-performance liquid chromatography (HPLC). Compared with the control reaction without enzyme, we saw consumption of caffeic acid and SAM, as measured by HPLC and TR-FRET, respectively, after 3 h of incubation (Figures 1A, S2A, and S2B). We observed a good correlation of the biological replicates within and across both detection methods with a slight overestimation of substrate consumption with the TR-FRET assay compared with HPLC detection. Later on we also achieved detection of SAM and SAH by HPLC (Figures S2C and S2D) and confirmed that there is no degradation of SAM over the course of the experiment in absence of an OMT enzyme or caffeic acid. In the MxSafC reaction, SAM appears to be consumed at a slightly higher rate than caffeic acid: 24.25% ± 0.16% of SAM and 18.11% ± 0.15% of caffeic acid are converted to their respective products within 24 h.

To address the cloning and expression bottleneck, we decided to use an *in vitro* transcription/translation expression platform, myTXTL from Arbor Bioscience (Ann Arbor, MI). This allowed us to express the genes of interest from synthetic, linear DNA fragments and saved us additional time for cloning, sequence verification, transformation, protein expression, and cell lysis (up to ~3 weeks of work). The linear DNA fragments were designed to contain the engineered p70a promoter (σ70) (Shin and Noireaux, 2010), a T500 terminator, and flanking overhangs of about 500 bp to protect from degradation in the myTXTL mix. Additionally, GamS protein was added to the reactions to protect the DNA fragments. We first tested the compatibility of the myTXTL reaction mix with the OMT assay and the TR-FRET detection method with MxSafC expressed from a linear template (Figure 1B). We performed two TXTL reactions at 29°C overnight and split them into three OMT reactions each. After stopping the OMT reactions, we analyzed them with the TR-FRET assay (two technical replicates) and HPLC. As negative controls we included two TXTL reactions that did not contain OMT-encoding DNA template (no technical replicates). Looking at the median of the data points, we again observe good correlation of the replicates within and across the detection methods; however, the TR-FRET assay appears to be more sensitive to experimental error than the HPLC

detection. The biological replicates of the enzyme expression (TXTL reactions 1 and 2) show only minor deviation, indicating that the experimental error in the expression step of the workflow is minimal.

Since we observed good correlation between the two detection methods yet low overall turnover yields, we proceeded with the established workflow with an extended incubation time for the OMT reaction (24 h) in later experiments.

Screening of putative OMTs for methylation of caffeic acid

To diversify our knowledge of OMTs in organisms other than plants, the premise of this study was to characterize a range of putative OMTs from various non-plant donor organisms across a relatively wide sequence landscape. Therefore, we first identified distantly related OMTs in the NCBI reference proteome database based on hidden Markov models (HMMs) (HMMsearch webtool, Potter et al., 2018) constructed from known plant caffeic acid OMTs (Joshi and Chiang, 1998; Liu et al., 2016) (search input 1, Table S1) and bacterial OMTs previously found to have a broad substrate tolerance toward catechols (Hou et al., 2007; Nelson et al., 2007; Kopycki et al., 2008; Youngdae et al., 2010) (search input 2). We found 15,994 unique sequences from all kingdoms of life, from ~190 Pfam families (Data S1). About 85% of the sequences were annotated as methyltransferases, more specifically 82% as OMTs, and about 10% contained dimerization domains. We filtered the sequences by length and alignment score and constructed a sequence similarity network to group them into clusters by pairwise amino acid sequence similarity (EFI-EST webtool, Gerlt et al., 2015). From those clusters, putative OMTs were chosen for experimental characterization (Table 1 and Figure S2) by taking the following criteria into consideration: the ranking of HMM scores within the clusters, a wide taxonomic spread over the selected enzymes, and a balanced selection of enzymes found with the two HMMsearch runs. Multiple enzymes were chosen from the major clusters, but some high-scoring putative OMTs were also picked from the smallest clusters.

The first large-scale screen of the selected putative OMTs was performed with caffeic acid as the substrate. We analyzed the enzymatic reactions by HPLC and TR-FRET (Figure S3) and repeated the experiment on a different day with a slightly different sample-handling workflow that allowed the consistent use of multi-channel pipettes throughout the experiment (Figure 2). The data points in the plots are ordered by increasing substrate turnover based on Figure 2A. The HPLC analysis shows a good correlation of the independent experiments with each other, both in relative terms (ranking of the tested enzyme by performance) and in absolute terms. This again indicates that the expression levels in the TXTL reactions are highly reproducible and that the technical error in the OMT reaction is low. However, for the TR-FRET analysis of the first experiment (Figure S2B), it is evident that the technical error by manual sample dilution and setup of the TR-FRET detection assay is very high (Figure S3B); therefore, the technical replicates deviate strongly. The overall noise of the experiment is very high, which becomes most apparent in the wells that appear to have higher SAM concentrations than the negative controls (here shown at the bottom of the plot). These experimental errors were overcome with a slightly different sample-handling procedure in the second experiment (Figure 2), which shows dramatically decreased noise in the data and a clear distinction between true and false positives. However, even in the first experiment with high background noise, the best-performing enzymes can be clearly distinguished from the other ones. In the intermediate range it is difficult to make a distinct cutoff. However, depending on the goal of this screening step, the cutoff can be set at a lower or higher level of SAM consumption at the risk of including false positives or excluding false negatives, respectively. In this case, we decided to make a very conservative cutoff and to even carry some true negatives forward to the characterization in *Escherichia coli* (vide infra). Overall, we observe a clear correlation between the HPLC and TR-FRET readout and were therefore encouraged to screen the enzymes against four other potential substrates: 1,2-dihydroxybenzene (catechol), ferulic acid, quercetin, and dopamine.

Screening of putative OMTs against other substrates

Next, we sought to use our *in vitro* expression and testing workflow to screen our panel of putative OMTs against other substrates. We selected catechol and dopamine (two known substrates for MxSafC and plant caffeic acid OMTs), quercetin (a flavonoid also often converted by plant caffeic acid OMTs), and ferulic acid (the precursor for a non-natural double-methylated product). We ran all reactions in parallel by diluting the TXTL reactions after overnight expression and aliquoting them into microtiter plates with the OMT reaction mixes. After 24 h we stopped the OMT reactions and assessed the SAM levels with the TR-FRET assay. We observed increased SAM consumption by 11 OMTs in the presence of catechol (Figure 3A) and by 15 OMTs in the presence of dopamine (Figure 3B), whereas in the presence of ferulic acid and quercetin only low levels of SAM conversion were observed that are difficult to separate from the background noise of the assay (Figures 3C and 3D). Although StrAOMT is reported to accept quercetin as a substrate (Youngdae et al., 2010), we did not observe any turnover. Since we did not have any true-positive controls for quercetin and ferulic acid in the panel of enzymes, we are inclined to interpret the results as negative for all enzymes. Also, in the presence of dopamine, the separation of positives and negatives is less clear-cut than with catechol. However, since the background noise appears to be rather small, we would suggest a more inclusive cutoff for further analysis.

Only considering the enzymes with highest SAM conversion, we see overlap in substrate acceptance for StyLOMT, RetFOMT, StrAOMT, OmnOMT, and MesMOMT. While the former enzymes show increased SAM conversion in the presence of all three substrates, MesMOMT does not consume SAM in the presence of dopamine. Several enzymes appear to display stronger substrate selectivity: KibPOMT and StiAOMT are selective for caffeic acid, HymGOMT, LegHOMT, MedSOMT, SapPOMT, SarHOMT, and SelSOMT are selective for catechol, and SalOMT is selective for dopamine. A sequence comparison of the tested OMTs shows that enzymes with similar activities also share higher sequence similarity with each other (Figure 4; software used: mafft v7.310 [Nakamura et al., 2018], FastTree v2.1.10 [Price et al., 2010], R packages ggplot2 and ggtree [Wickham, 2011; Yu et al., 2018]). Looking at the active-site residues predicted

Table 1. List of putative OMTs selected for experimental characterization

Protein name in this study	UniProt name	Donor organism	Domain	Phylum (class)	HMMsearch E-value	HMMsearch Score	Catalytic triad
HMMsearch 1 (plant caffeic acid OMTs as seed sequences)							H-E-E
AlkOMT	A0A251WJU7_9CYAN	*Alkalinema* sp. CACIAM 70d	Bacteria	Cyanobacteria (Melainabacteria group)	4.10E-44	162	H-E-E
BraLOMT	A0A0R3MQ32_9BRAD	*Bradyrhizobium lablabi*	Bacteria	Proteobacteria (alpha)	2.10E-33	126.7	H-E-E
BucROMT	A0A091HDB2_BUCRH	*Buceros rhinoceros silvestris*	Eukaryota	Metazoa	5.70E-27	105.6	H-E-E
CanNOMT	A0A0N9Y1E2_9ARCH	*Candidatus nitrocosmicus oleophilus*	Archaea	Thaumarchaeota	4.90E-32	122.2	H-E-E
CreAOMT	A0A1Q7MH91_9CREN	*Crenarchaeota archaeon* 13_1_40CM_3_52_17	Archaea	Crenarchaeota	7.50E-31	118.3	H-G-E
DicDOMT	OMT12_DICDI	*Dictyostelium discoideum*	Eukaryota	Mycetozoa	7.70E-31	118.3	H-D-E
GloKOMT	U5QFM0_9CYAN	*Gloeobacter kilaueensis* JS1	Bacteria	Cyanobacteria (Melainabacteria group)	4.20E-45	165.2	S-E-E
GloOMT	K9XAK2_9CHRO	*Gloeocapsa* sp. PCC 7428	Bacteria	Cyanobacteria (Melainabacteria group)	7.80E-37	138	H-Q-W
HalOMT	U1MFJ5_9EURY	halophilic archaeon J07HX5	Archaea	Halobacteria	5.60E-30	115.4	H-E-E
HymGOMT	A0A212T1X1_9BACT	*Hymenobacter gelipurpurascens*	Bacteria	Bacteroidetes (Chlorobi group)	7.70E-42	154.5	H-E-E
LegHOMT	A0A0A8UVF9_LEGHA	*Legionella hackeliae*	Bacteria	Gammaproteobacteria	9.50E-29	111.4	H-E-Q
MesMOMT	A0A1G9C2B4_9RHIZ	*Mesorhizobium muleiense*	Bacteria	Alphaproteobacteria	9.40E-34	127.9	H-E-E
SapPOMT	A0A067BNB9_SAPPC	*Saprolegnia parasitica* (strain CBS 223.65)	Eukaryota	Oomycetes	3.70E-28	109.5	H-D-E
TieLOMT	A0A151ZKG1_9MYCE	*Tieghemostelium lacteum*	Eukaryota	Mycetozoa	5.50E-28	108.9	H-D-E
HMMsearch 2 (bacterial OMTs as seed sequences)							K-N-D
AciOMT	A0A178GH82_9GAMM	*Acinetobacter* sp. SFD	Bacteria	Gammaproteobacteria	5.60E-27	105.4	R-N-A
ChiCOMT	A0A1M6USV2_9FLAO	*Chishuiella changwenlii*	Bacteria	Bacteroidetes (Chlorobi group)	2.20E-54	195	K-N-D
DesAOMT	Q1JXV1_DESA6	*Desulfuromonas acetoxidans* (strain DSM 684)	Bacteria	Proteobacteria (delta/epsilon)	3.70E-30	115.8	R-N-K
KibpOMT	A0A0N9HPV5_9PSEU	*Kibdelosporangium phytohabitans*	Bacteria	Actinobacteria	5.10E-41	151.3	K-N-D
OmnOMT	A0A1G1JPP6_9BACT	*Omnitrophica bacterium* GWA2_52_8	Bacteria	(PVC group) Candidatus Omnitrophica	2.40E-54	194.9	K-N-D
PhoAOMT	A0A1U7IJN5_9CYAN	*Phormidium ambiguum* IAM M-71	Bacteria	Cyanobacteria (Melainabacteria group)	2.00E-93	322.7	K-N-D
RetFOMT	X6M5Z7_RETFI	*Reticulomyxa filosa*	Eukaryota	Foraminifera	4.90E-54	193.9	K-N-D
SalOMT	R4W9N9_9EURY	*Salinarchaeum* sp. Harcht-Bsk1	Archaea	Halobacteria	2.30E-25	100.1	K-N-D
SarHOMT	G3WFI7_SARHA	*Sarcophilus harrisii*	Eukaryota	Metazoa	2.80E-54	194.7	K-N-D
SelSOMT	A0A1T4QLE1_9FIRM	*Selenihalanaerobacter shriftii*	Bacteria	Firmicutes	2.90E-42	155.4	K-N-D
StiAOMT	E3FEM3_STIAD	*Stigmatella aurantiaca*	Bacteria	Proteobacteria (delta/epsilon)	6.20E-20	82.4	K-N-S
StyLOMT	A0A078AUZ0_STYLE	*Stylonychia lemnae*	Eukaryota	Ciliophora	2.40E-54	194.9	K-N-D
TheMOMT	E6SHY4_THEM7	*Thermaerobacter marianensis* (strain ATCC 700841)	Bacteria	Firmicutes	6.90E-64	226.1	K-N-D
VerLOMT	A0A0G4MCD6_9PEZI	*Verticillium longisporum*	Eukaryota	Fungi	7.00E-21	85.5	K-N-D

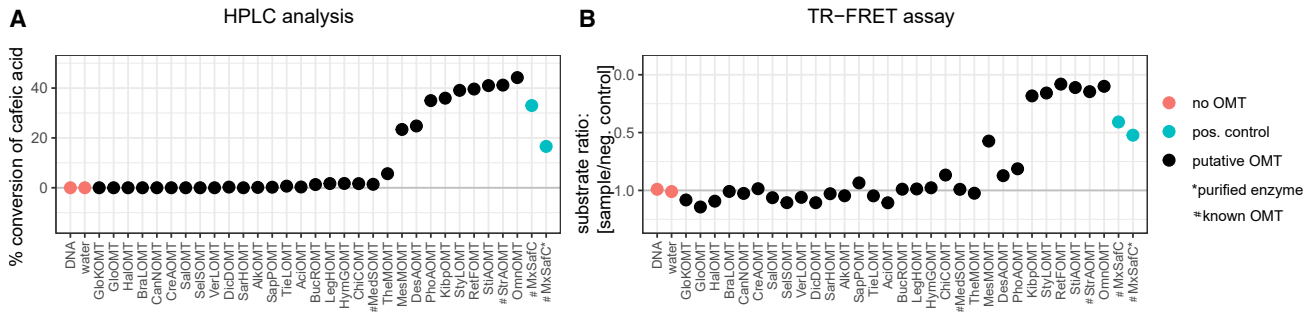

Figure 2. Screening of 30 enzymes of interest against caffeic acid as substrate and SAM as co-substrate

OMT reaction was stopped after 24 h.

(A) Samples analyzed by HPLC, expressed as percent caffeic acid converted (c_0[caffeic acid] = 2 mM).

(B) Samples analyzed by TR-FRET expressed as SAM levels detected relative to the "no OMT" controls (c_0[SAM] = 2 mM).

Data points represent single measurements and are sorted by increasing substrate turnover based on (B). Red data points, negative controls; blue data points, positive controls. See also Figure S3 for an independent replicate of this experiment and Figure S5 for visualization of enzyme expression by SDS-PAGE.

on the basis of multiple sequence alignments, we see that some of the tested OMTs display activity although they carry changes in the putative catalytic triad (Table 1). In the group of enzymes from HMMsearch 1 (plant input sequences), the catalytic triad should be H-E-E (in *Medicago sativa* COMT1_MEDSA residues H269, E297, and E329 [Zubieta et al., 2002]) and is highly conserved with a few exceptions—CreAOMT, GloKOMT, GloOMT, LegHOMT—with all enzymes being active. In the group of enzymes from HMMsearch 2 (bacterial input sequences), the catalytic triad should be K-N-D (in MxSafC residues K145, N69, D212 [Brandt et al., 2015]) and is even more conserved. Only three sequences—AciOMT, DesAOMT, and StiAOMT—show significant changes in these amino acids, with only AciOMT being inactive. This suggests that there must be other changes in the active-site architecture of these OMTs that compensate for these amino acid substitutions. With a stricter pre-selection based on sequence similarity and active-site conservation, we might have missed these interesting OMTs, whereas our pre-screening approach enabled us to explore a wider sequence space.

Application of pre-screened OMTs in a pathway toward (iso-)ferulic acid

Lastly, we sought to use the pre-screened OMTs in an *E. coli* microbial cell factory. We chose to expand our previously constructed and optimized pathway from tyrosine to caffeic acid (Rodrigues et al., 2015; Haslinger and Prather, 2020) by one enzymatic step in order to generate the pharmaceutically relevant phenolic acid ferulic acid, and its regio-isomer 4-methoxy-3-hydroxy-cinnamic acid (iso-ferulic acid). To select enzymes for testing in the recombinant pathway, we first explored the data from the pre-screening assay in the context of enzyme expression, protein sequence, and the donor organism. We found that the presence or absence of a band of the appropriate size in the SDS-PAGE did not correlate with observed enzymatic activity (Figure S5). For instance, in the lane of one of the best-performing enzymes, StyLOMT, we did not see a distinct band on SDS-PAGE, whereas for some inactive enzymes such as HalOMT we saw a distinct band on SDS-PAGE. This indicates that some enzymes are expressed at a low level and yet are active, whereas others are either not correctly expressed and folded, or were simply not challenged with the appropriate substrate in this study. When mapping the pre-screening results onto the sequence similarity network, we notice that the enzymes active on caffeic acid (Figure S4, filled symbols) are distributed across the network, with most of them being part of the main cluster. All active OMTs except MesMOMT show highest sequence similarity with the bacterial seed sequences (Figure S4, yellow boxes). This indicates that the bacterial input sequences provided a better search template for identifying new caffeic acid OMTs than the plant input sequences. Since some of the putative OMTs found with the plant input sequences display activity against catechol and dopamine, we can exclude that the lack of activity on caffeic acid is caused by a general problem with our *in silico* selection, *in vitro* expression, and pre-screening approach. However, for the putative OMTs that did not display activity on any of the tested substrates, we cannot rule out protein expression and folding problems. Two of the active enzymes, RetFOMT and StyLOMT, are from eukaryotic donors and the rest are from bacterial donors. This indicates that the pre-screening method is also applicable to eukaryotic enzymes.

Based on the pre-screening results, we chose the ten top-performing enzymes including the previously characterized StrAOMT (Youngdae et al., 2010) and MxSafC (Nelson et al., 2007; Siegrist et al., 2017) and two enzymes that were inactive in the pre-screen: HalOMT (archaeal donor, visibly expressed) and SalOMT (archaeal donor, not visibly expressed). We cloned the respective genes into the vector pRSFduet:FjTAL, which already contained the tyrosine ammonia lyase gene from *Flavobacterium johnsoniae* (FjTAL, first pathway step) in a separate expression cassette, for expression under the T7 promoter (Table S2). We co-transformed each new plasmid with two other plasmids encoding for the cytochrome P450 monooxygenase CYP199A2 F185L NΔ7 and its redox partners (second pathway step) from our previous study (Haslinger and Prather, 2020) into *E. coli* K12 MG1655DE3. In the resulting strains (s01-s12, Table S3) L-tyrosine will be converted to *p*-coumaric acid by FjTAL, to caffeic acid by CYP199A2 F185L NΔ7, and to (iso-) ferulic acid by the OMTs. As a negative control, we used a strain

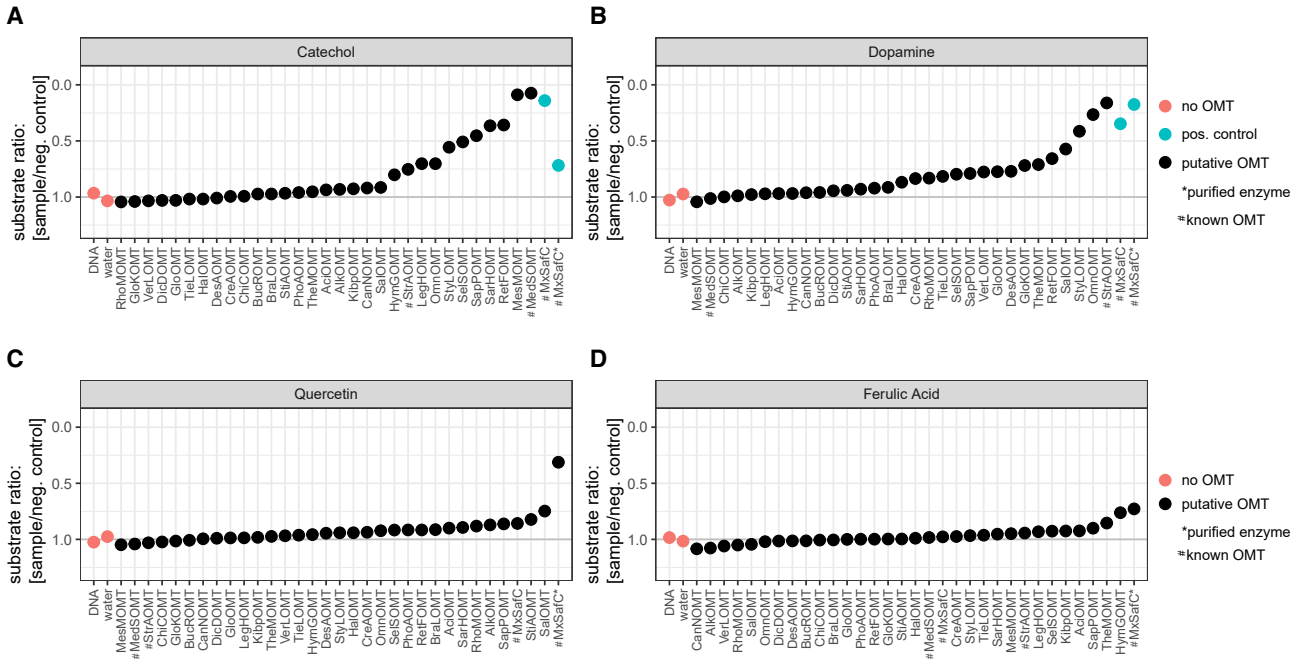

Figure 3. Screening for OMT activity of all enzymes of interest *in vitro* with four different substrates

Catechol (A), dopamine (B), quercetin (C), and ferulic acid (D). Samples analyzed by TR-FRET expressed as SAM levels detected relative to the "no OMT" controls (c_0[SAM] = 2 mM). Data points ordered by increasing substrate conversion for each panel from left to right; Red data points, negative controls; blue data points, positive controls (if available). See also Figure S1 for a schematic representation of the respective substrates.

with the pRSF:FjTAL plasmid lacking an OMT gene (s00). In initial fermentation experiments with the modified M9 minimal medium composition that we had previously used (Haslinger and Prather, 2020), we did not observe significant product formation from glucose or fed L-tyrosine (data not shown), and therefore decided to first optimize the conditions for the OMT catalyzed step with a subset of the strains and in smaller-scale reactions with fed caffeic acid. We observed that the addition of Mg^{2+} (obligate co-factor for certain OMTs) by itself only led to slightly higher caffeic acid conversion, whereas feeding of L-methionine as a precursor for SAM improved the turnover by 2.2- to 3.6-fold (Figure 5A). This finding is consistent with previous observations for vanillin biosynthesis in *E. coli* (Kunjapur et al., 2016) and indicates that SAM supply is limited and needs to be increased for OMT-containing pathways to be efficient. With this knowledge, we tested all strains in 15-mL fermentations with glucose as a carbon source, L-tyrosine as a pathway precursor, and Mg^{2+} and L-methionine as additives for the OMT reaction. We observed product formation for all strains expressing OMTs that had tested active in the pre-screening step (Figure 5B). In most strains more than half of the caffeic acid formed was converted to the methylated products, and four strains even achieved full conversion: s06 expressing PhoAOMT, s08 expressing StyLOMT, s09 expressing RetFOMT and s11 expressing StrAOMT. In terms of titers, s11 displays the most desirable outcome with low titers for pathway intermediates and side products, and a high product titer of 0.49 ± 0.06 mM (Figure 5C). Interestingly, all OMTs displayed a strong regioselectivity for the *meta* position over the *para* position *in vivo*, although some showed a preference for the *para* position in the *in vitro* screening step (Table S4). It is difficult to rationalize this phenomenon, but several factors could play a role. The first factor to consider is that the concentrations of enzymes, substrate, and co-factors are different from those in the *in vitro* assay and likely fluctuate over time depending on synthesis rate (enzyme, caffeic acid, and SAM) and uptake rate (Mg^{2+}). More importantly, however, it has been shown that for those enzymes utilizing divalent cations, the presence of other cations and the pH of the reaction can have a strong influence on the regioselectivity (Senoh et al., 1962; Siegrist et al., 2017). The cytosolic pH of *E. coli* should be slightly higher than the pH of the *in vitro* reaction (pH 7.2–7.8 versus pH 7.0), and several cations are present in the cell. While this observation indicates that *in vitro* data cannot necessarily be directly translated into whole-cell applications, our pre-screening step decreased the experimental load for cloning, fermentation, and product analysis by HPLC by at least two-thirds. The pre-screening step itself for 30 enzymes against five substrates took 3 days: day 1, preparation of TXTL reactions (1 h hands-on time, 16 h incubation); day 2, preparation of OMT reactions (1–2 h hands-on-time, 24 h incubation); day 3, TR-FRET assay (1 h hands-on time, 1 h for incubation and readout, 1 h for result analysis). Using HPLC detection for the same number of samples (>200 including controls and analytical standards, excluding method development) would have required more than 100 h of instrument time with our equipment. Cloning of the plasmids for *in vivo* testing took about 3 weeks and would have likely taken longer with a larger number of genes to be cloned. The fermentation experiment followed by HPLC analysis

Figure 4. Summary of observed enzyme activities mapped onto a phylogenetic tree

The phylogenetic tree on the left was calculated based on a multiple sequence alignment of the enzymes screened in this study and the HMMsearch input sequences (green: HMMsearch1; yellow: HMMsearch 2). *In vitro* activity data on caffeic acid, catechol, and dopamine are shown as colored boxes on the right (dark color indicates *in vitro* activity observed). See also Figure S4 for mapping of the experimental data onto the sequence similarity network used to select the OMTs for this study.

required about 2 weeks of time (1 week for fermentation, 1 week for HPLC analysis) and, without investment into a different cultivation setup, this time would have tripled had we not used the pre-screen to eliminate two-thirds of the enzymes in the panel.

The best-performing OMT, StrAOMT, had previously been observed to act on caffeic acid, though with low catalytic efficiency (Youngdae et al., 2010). To our surprise it was one of the top performers in the pre-screening and the pathway application in this study. To the best of our knowledge, StrAOMT has not been used previously in the context of a pathway.

DISCUSSION

Closing the gap between computational annotations and the biotechnological exploitation of natural enzymes as industrial biocatalysts requires extensive functional screening of enzyme libraries. Alternatively, scarce sampling of enzyme families and deep functional analysis ("thick data") can be utilized to improve annotation pipelines and, thus, the interpretation of "big data." In this study, we developed a rapid prototyping platform for SAM-dependent methyltransferases, an enzyme superfamily that has great potential for functionalization of natural product-inspired pharmaceuticals. The chosen approach follows in the footsteps of a range of studies utilizing *in vitro* transcription/translation systems for prototyping of antibodies (Yin et al., 2012), protein expression enhancing factors (Woodrow and Swartz, 2007), transcription regulatory elements (McManus et al., 2019), G-protein-coupled receptors (Cortès et al., 2019), quorum-sensing systems (Halleran and Murray, 2018), glycosyltransferases (Lin et al., 2020; Techner et al., 2020), and entire biosynthetic pathways (Zhu et al., 2014; Toogood et al., 2015; Kelwick et al., 2018; Dudley et al., 2019; O'Kane et al., 2019; Karim et al., 2020; Khatri et al., 2020; Lai et al., 2020), which highlights the generalizability of this expression system (Dopp et al., 2019). In our study we observed that the enzymatic activity is highly reproducible across biological replicates of the *in vitro* transcription/translation system, which is in good agreement with the previous studies. In addition to the time and effort saved on molecular cloning, transformation, and protein expression in *E. coli* (1–3 weeks), another advantage is that no additional lysis and clearing steps are required before the enzymatic reaction is performed. This is particularly advantageous for enzymes requiring co-factors that cannot cross the cell membrane, such as SAM. In our workflow, we combined the *in vitro* expression system with a microliter-scale enzymatic assay coupled to a TR-FRET readout that we used as a qualitative (activity/no activity) assessment. While this readout is sensitive to experimental error due to the small volumes and the required dilution steps, we were able to generate robust results by using master mixes and multichannel pipettes for all steps. The TR-FRET-based detection of the SAM co-factor, rather than a specific substrate or product, allows for the screening of a library of substrates. The format can furthermore be used to swiftly optimize reaction conditions, such as buffers, salts, and substrate concentrations, and thus generate "thick data." The entire workflow should be amenable to automation by using liquid-handling robots and is therefore scalable to also screen large

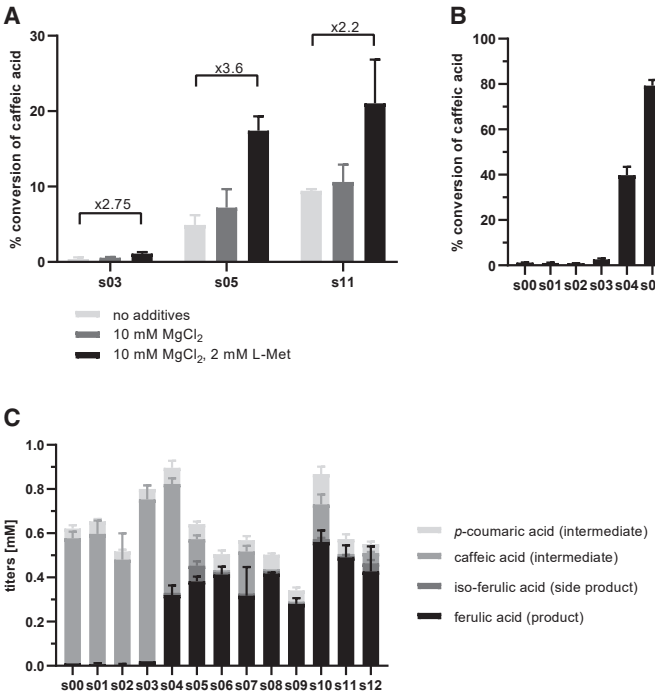

Figure 5. Fermentation products of *E. coli* K12 MG1655(DE3) expressing a recombinant pathway to produce (iso-)ferulic acid

(A) Media optimization performed with feeding of the pathway intermediate caffeic acid (2 mM); data displayed as percent conversion of fed caffeic acid. (B and C) Experiment performed with optimized media with glucose as a carbon source and L-tyrosine (3 mM) as a pathway precursor. Data are displayed as percent conversion of produced caffeic acid (B) or as stacked histogram of titers of product, side product, and pathway intermediates (C). Data represent mean ± SD of three biological replicates. See also Table S4 for regioselectivity of the OMTs.

enzyme libraries. The fact that commercial kits were used for the entire workflow makes the approach also useful for laboratories with no prior experience with *in vitro* transcription/translation systems and without access to high-throughput and high-resolution analytics. This comes at the cost of possibly overlooking enzymes that cannot be functionally expressed in sufficient levels in the myTXTL kit. It remains up to the scientists to weigh their options depending on the goal of their study.

The workflow allowed us to rapidly screen ~30 enzymes against five substrates. Particularly for caffeic acid as a substrate, we identified several distant homologs with remarkable activity, two of which do not even carry the conserved active-site residues. With a more conservative *in silico* approach of selecting enzymes of interest, we might not even have considered these as suitable enzymes. However, our approach allowed us to cast a wide net, explore the activity of these distantly related enzymes and use them in an *E. coli* cell factory for ferulic acid, a methylated phenolic acid of pharmaceutical interest. Zooming in on these unexpected hits and their close relatives with structural and functional studies will allow us to better understand the underlying mechanisms of substrate selectivity and regioselectivity in OMTs.

Lastly, we tested a subset of the pre-screened OMTs in the context of a recombinant biosynthetic pathway in *E. coli*. We observed that all enzymes seen to be active in the pre-screening step were also catalytically active in the pathway, whereas enzymes found to be inactive in the screen remained inactive in the pathway. The trends in substrate conversion levels and regioselectivity, however, were not necessarily correlated between the *in vitro* and *in vivo* experiments. This is a hurdle well known to metabolic engineers and is inherent to *in vitro* characterization of enzymes. However, the high cost of *in vivo* screening in terms of time and consumables justifies the need for *in vitro* prototyping.

SIGNIFICANCE

Methyl groups on natural and synthetic small molecules are important for their chemical and biological properties. In manufacturing, these groups can be introduced with methyltransferase enzymes in an elegant and environmentally friendly fashion. However, identifying enzymes with the appropriate substrate specificity among thousands of putative enzymes in databases is a tedious and time-consuming process. To overcome this bottleneck, we developed a rapid workflow to screen a library of enzymes against a range of substrates. We used the workflow to pre-screen oxygen-directed methyltransferases from a wide range of organisms and demonstrated the direct application of the best-performing enzymes in a recombinant pathway in *Escherichia coli*. This study opens the door to a more comprehensive understanding of the relationship between amino acid sequence and enzymatic function of this important enzyme family and provides several active enzymes that can be further explored for biomanufacturing. The screening method is based on a microliter-scale plate assay and is highly amenable to automation. It should be universally applicable to all methyltransferases utilizing *S*-adenosylmethionine as a cofactor without major adaptations.

STAR★METHODS

Detailed methods are provided in the online version of this paper and include the following:

- KEY RESOURCES TABLE
- RESOURCE AVAILABILITY

SUPPLEMENTAL INFORMATION

Supplemental information can be found online at https://doi.org/10.1016/j.chembiol.2021.04.010.

AUTHOR CONTRIBUTIONS

K.H. conceived the study, selected the putative OMTs, performed all experiments, and wrote the manuscript with support and guidance from K.L.J.P. K.H. and T.H. analyzed the data and created figures. T.H. provided bioinformatics support. All authors read and approved the final version of the manuscript.

ACKNOWLEDGMENTS

K.H. is grateful for the support by the Human Frontier Science Program (grant number LT000969/2016-L). This work was supported by the MIT Portugal Program (grant number 6937822).

DECLARATION OF INTERESTS

The authors declare no competing interests.

Received: September 27, 2020
Revised: February 20, 2021
Accepted: April 16, 2021
Published: May 5, 2021

REFERENCES

Brandt, W., Manke, K., and Vogt, T. (2015). A catalytic triad—Lys-Asn-Asp—is essential for the catalysis of the methyl transfer in plant cation-dependent O-methyltransferases. Phytochemistry *113*, 130–139, https://doi.org/10.1016/j.phytochem.2014.12.018.

Casini, A., Chang, F.-Y., Eluere, R., King, A.M., Young, E.M., Dudley, Q.M., Karim, A., Pratt, K., Bristol, C., Forget, A., et al. (2018). A pressure test to make 10 molecules in 90 days: external evaluation of methods to engineer biology. J. Am. Chem. Soc. *140*, 4302–4316, https://doi.org/10.1021/jacs.7b13292.

Chao, R., Mishra, S., Si, T., and Zhao, H. (2017). Engineering biological systems using automated biofoundries. Metab. Eng. *42*, 98–108, https://doi.org/10.1016/j.ymben.2017.06.003.

Cortès, S., Hibti, F.E., Chiraz, F., and Ezzine, S. (2019). High-throughput *E. coli* cell-free expression: from PCR product design to functional validation of GPCR. Methods Mol. Biol. *2025*, 261–279, https://doi.org/10.1007/978-1-4939-9624-7_12.

Das, D., Khan, H.P.A., Shivahare, R., Gupta, S., Sarkar, J., Siddiqui, M.I., Sankar Ampapathi, R., and Chakraborty, T.K. (2017). Synthesis, SAR and biological studies of sugar amino acid-based almiramide analogues: N-methylation leads the way. Org. Biomol. Chem. *15*, 3337, https://doi.org/10.1039/c6ob02610a.

Dopp, J.L., Rothstein, S.M., Mansell, T.J., and Reuel, N.F. (2019). Rapid prototyping of proteins: mail order gene fragments to assayable proteins within 24 hours. Biotechnol. Bioeng. *116* (3), 667–676, https://doi.org/10.1002/bit.26912.

Dudley, Q.M., Nash, C.J., and Jewett, M.C. (2019). Cell-free biosynthesis of limonene using enzyme-enriched *Escherichia coli* lysates. Synth. Biol. *4* (1), ysz003, https://doi.org/10.1093/SYNBIO/YSZ003.

Finkle, B.J., and Nelson, R.F. (1963). Enzyme reactions with phenolic compounds: a meta-O-methyltransferase in plants. Biochim. Biophys. Acta *78*, 747–749.

Garamella, J., Marshall, R., Rustad, M., and Noireaux, V. (2016). The all *E. coli* TX-TL toolbox 2.0: a platform for cell-free synthetic biology. ACS Synth. Biol. *5* (4), 344–355, https://doi.org/10.1021/acssynbio.5b00296.

Gerlt, J.A., Bouvier, J.T., Davidson, D.B., Imker, H.J., Sadkhin, B., Slater, D.R., and Whalen, K.L. (2015). Enzyme Function Initiative-Enzyme Similarity Tool (EFI-EST): a web tool for generating protein sequence similarity networks. Biochim. Biophys. Acta *1854* (8), 1019–1037, https://doi.org/10.1016/j.bbapap.2015.04.015.

Halleran, A.D., and Murray, R.M. (2018). Cell-free and in vivo characterization of Lux, Las, and Rpa quorum activation systems in *E. coli*. ACS Synth. Biol. *7* (2), 752–755, https://doi.org/10.1021/acssynbio.7b00376.

Haslinger, K., and Prather, K.L.J. (2020). Heterologous caffeic acid biosynthesis in *Escherichia coli* is affected by choice of tyrosine ammonia lyase and redox partners for bacterial cytochrome P450. Microb. Cell Fact. *19*, 26, https://doi.org/10.1101/707828.

Heyduk, T., and Heyduk, E. (2002). Molecular beacons for detecting DNA binding proteins. Nat. Biotechnol. *20* (2), 171–176, https://doi.org/10.1038/nbt0202-171.

Hicks, M.a., and Prather, K.L.J. (2014). Bioprospecting in the genomic age. Adv. Appl. Microbiol. *87*, 111–146, https://doi.org/10.1016/B978-0-12-800261-2.00003-7.

Higuchi, T., Shimada, M., Nakatsubo, F., and Tanahashi, M. (1977). Differences in biosyntheses of guaiacyl and syringyl lignins in woods. Wood Sci. Technol. *11*, 153–167.

Hou, X., Wang, Y., Zhou, Z., Bao, S., Lin, Y., and Gong, W. (2007). Crystal structure of SAM-dependent O-methyltransferase from pathogenic bacterium *Leptospira interrogans*. J. Struct. Biol. *159* (3), 523–528, https://doi.org/10.1016/J.JSB.2007.04.007.

Inoue, H., Nojima, H., and Okayama, H. (1990). High efficiency transformation of *Escherichia coli* with plasmids. Gene *96* (1), 23–28, https://doi.org/10.1016/0378-1119(90)90336-P.

Jacques, P., Béchet, M., Bigan, M., Caly, D., Chataigné, G., Coutte, F., Flahaut, C., Heuson, E., Leclère, V., Lecouturier, D., et al. (2017). High-throughput strategies for the discovery and engineering of enzymes for biocatalysis. Bioproc. Biosyst. Eng. *40*, 161–180, https://doi.org/10.1007/s00449-016-1690-x.

Joshi, C.P., and Chiang, V.L. (1998). Conserved sequence motifs in plant S-adenosyl-L-methionine-dependent methyltransferases. Plant Mol. Biol. *37* (4), 663–674, https://doi.org/10.1023/A:1006035210889.

Kadoma, Y., and Fujisawa, S. (2008). A comparative study of the radical-scavenging activity of the phenolcarboxylic acids caffeic acid, p-coumaric acid, chlorogenic acid and ferulic acid, with or without 2-mercaptoethanol, a thiol, using the induction period method. Molecules *13* (10), 2488–2499, https://doi.org/10.3390/molecules13102488.

Karim, A.S., Dudley, Q.M., Juminaga, A., Yuan, Y., Crowe, S.A., Heggestad, J.T., Garg, S., Abdalla, T., Grubbe, W.S., Rasor, B.J., et al. (2020). In vitro prototyping and rapid optimization of biosynthetic enzymes for cell design. Nat. Chem. Biol. *16* (8), 912–919, https://doi.org/10.1038/s41589-020-0559-0.

Kelwick, R., Ricci, L., Chee, S.M., Bell, D., Webb, A.J., and Freemont, P.S. (2018). Cell-free prototyping strategies for enhancing the sustainable production of polyhydroxyalkanoates bioplastics. Synth. Biol. *3* (1), 1–12, https://doi.org/10.1093/synbio/ysy016.

Khatri, Y., Hohlman, R.M., Mendoza, J., Li, S., Lowell, A.N., Asahara, H., and Sherman, D.H. (2020). Multicomponent microscale biosynthesis of unnatural cyanobacterial indole alkaloids. ACS Synth. Biol. *9* (6), 1349–1360, https://doi.org/10.1021/acssynbio.0c00038.

Koirala, N., Thuan, N.H., Ghimire, G.P., Thang, D. Van, and Sohng, J.K. (2016). Methylation of flavonoids: chemical structures, bioactivities, progress and perspectives for biotechnological production. Enzyme Microb. Technol. *86*, 103–116, https://doi.org/10.1016/j.enzmictec.2016.02.003.

Kopycki, J.G., Stubbs, M.T., Brandt, W., Hagemann, M., Porzel, A., Schmidt, J., Schliemann, W., Zenk, M.H., and Vogt, T. (2008). Functional and structural characterization of a cation-dependent O-methyltransferase from the cyanobacterium *Synechocystis* sp. strain PCC 6803. J. Biol. Chem. *283*, 20888–20896, https://doi.org/10.1074/jbc.M801943200.

Kunjapur, A.M., Hyun, J.C., and Prather, K.L.J. (2016). Deregulation of S-adenosylmethionine biosynthesis and regeneration improves methylation in the *E. coli* de novo vanillin biosynthesis pathway. Microb. Cell Fact. *15*, 61, https://doi.org/10.1186/s12934-016-0459-x.

Lai, H.E., Obled, A.M.C., Chee, S.M., Morgan, R.M., Sharma, S.V., Moore, S.J., Polizzi, K.M., Goss, R.J.M., and Freemont, P.S. (2020). A GenoChemetic strategy for derivatization of the violacein natural product scaffold. bioRxiv. https://doi.org/10.1101/202523.

Li, Y., Bionda, N., Yongye, A., Geer, P., Stawikowski, M., Cudic, P., Martinez, K., and Houghten, R.A. (2013). Dissociation of antimicrobial and hemolytic activities of gramicidin S through N-methylation modification. ChemMedChem *8*, 1865–1872, https://doi.org/10.1002/cmdc.201300232.

Lin, L., Kightlinger, W., Prabhu, S.K., Hockenberry, A.J., Li, C., Wang, L.-X., Jewett, M.C., and Mrksich, M. (2020). Sequential glycosylation of proteins with substrate-specific N-glycosyltransferases. ACS Cent. Sci. *6* (2), 144–154, https://doi.org/10.1021/acscentsci.9b00021.

Liscombe, D.K., Louie, G.V., and Noel, J.P. (2012). Architectures, mechanisms and molecular evolution of natural product methyltransferases. Nat. Prod. Rep. *29* (10), 1238, https://doi.org/10.1039/c2np20029e.

Liu, X., Luo, Y., Wu, H., Xi, W., Yu, J., Zhang, Q., and Zhou, Z. (2016). Systematic analysis of O-methyltransferase gene family and identification of potential members involved in the formation of O-methylated flavonoids in *Citrus*. Gene *575* (2), 458–472, https://doi.org/10.1016/j.gene.2015.09.048.

Longwell, C.K., Labanieh, L., and Cochran, J.R. (2017). High-throughput screening technologies for enzyme engineering. Curr. Opin. Biotechnol. *48*, 196–202, https://doi.org/10.1016/j.copbio.2017.05.012.

McManus, J.B., Emanuel, P.A., Murray, R.M., and Lux, M.W. (2019). A method for cost-effective and rapid characterization of engineered T7-based transcription factors by cell-free protein synthesis reveals insights into the regulation of T7 RNA polymerase-driven expression. Arch. Biochem. Biophys. *674*, 108045, https://doi.org/10.1016/j.abb.2019.07.010.

Nakamura, T., Yamada, K.D., Tomii, K., and Katoh, K. (2018). Parallelization of MAFFT for large-scale multiple sequence alignments. Bioinformatics *34* (14), 2490–2492, https://doi.org/10.1093/bioinformatics/bty121.

Nelson, J.T., Lee, J., Sims, J.W., and Schmidt, E.W. (2007). Characterization of SafC, a catechol 4-O-methyltransferase involved in saframycin biosynthesis. Appl. Environ. Microbiol. *73* (11), 3575–3580, https://doi.org/10.1128/AEM.00011-07.

Nielsen, D.R., Yoon, S.-H., Yuan, C.J., and Prather, K.L.J. (2010). Metabolic engineering of acetoin and meso-2, 3-butanediol biosynthesis in *E. coli*. Biotechnol. J. *5* (3), 274–284, https://doi.org/10.1002/biot.200900279.

O'Kane, P.T., Dudley, Q.M., McMillan, A.K., Jewett, M.C., and Mrksich, M. (2019). High-throughput mapping of CoA metabolites by SAMDI-MS to optimize the cell-free biosynthesis of HMG-CoA. Sci. Adv. *5* (6), eaaw9180, https://doi.org/10.1126/sciadv.aaw9180.

Potter, S.C., Luciani, A., Eddy, S.R., Park, Y., Lopez, R., and Finn, R.D. (2018). HMMER web server: 2018 update. Nucleic Acids Res. *46*, W200–W204, https://doi.org/10.1093/nar/gky448.

Price, M.N., Dehal, P.S., and Arkin, A.P. (2010). FastTree 2—approximately maximum-likelihood trees for large alignments. PLoS One *5*, e9490, https://doi.org/10.1371/journal.pone.0009490.

Rodrigues, J.L., Araújo, R.G., Prather, K.L.J., Kluskens, L.D., and Rodrigues, L.R. (2015). Heterologous production of caffeic acid from tyrosine in *Escherichia coli*. Enzyme Microb. Technol. *71*, 36–44, https://doi.org/10.1016/j.enzmictec.2015.01.001.

Senoh, S., Tokuyama, Y., and Witkop, B. (1962). The role of cations in non-enzymatic and enzymatic O-methylations of catechol derivatives. J. Am. Chem. Soc. *84* (9), 1719–1724, https://doi.org/10.1021/ja00868a045.

Shannon, P., Markiel, A., Ozier, O., Baliga, N.S., Wang, J.T., Ramage, D., Amin, N., Schwikowski, B., and Ideker, T. (2003). Cytoscape: a software environment for integrated Models. Genome Res. *13* (11), 2498–2504, https://doi.org/10.1101/gr.1239303.metabolite.

Shin, J., and Noireaux, V. (2010). Efficient cell-free expression with the endogenous *E. coli* RNA polymerase and sigma factor 70. J. Biol. Eng. *4* (1), 8, https://doi.org/10.1186/1754-1611-4-8.

Siegrist, J., Netzer, J., Mordhorst, S., Karst, L., Gerhardt, S., Einsle, O., Richter, M., and Andexer, J.N. (2017). Functional and structural characterisation of a bacterial O -methyltransferase and factors determining regioselectivity. FEBS Lett. *591* (2), 312–321, https://doi.org/10.1002/1873-3468.12530.

Sievers, F., Wilm, A., Dineen, D., Gibson, T.J., Karplus, K., Li, W., Lopez, R., McWilliam, H., Remmert, M., Söding, J., et al. (2011). Fast, scalable generation of high-quality protein multiple sequence alignments using Clustal Omega. Mol. Syst. Biol. *7* (1), 539, https://doi.org/10.1038/msb.2011.75.

Taram, F., Winter, A.N., and Linseman, D.A. (2016). Neuroprotection comparison of chlorogenic acid and its metabolites against mechanistically distinct cell death-inducing agents in cultured cerebellar granule neurons. Brain Res. *1648*, 69–80, https://doi.org/10.1016/j.brainres.2016.07.028.

Techner, J.-M., Kightlinger, W., Lin, L., Hershewe, J., Ramesh, A., DeLisa, M.P., Jewett, M.C., and Mrksich, M. (2020). High-throughput synthesis and analysis of intact glycoproteins using SAMDI-MS. Anal. Chem. *92* (2), 1963–1971, https://doi.org/10.1021/acs.analchem.9b04334.

Tian, L., Wang, R.E., Fei, Y., and Chang, Y.-H. (2012). A homogeneous fluorescent assay for cAMP-phosphodiesterase enzyme activity. J. Biomol. Screen. *17* (3), 409–414, https://doi.org/10.1177/1087057111426901.

Toogood, H.S., Cheallaigh, A.N., Tait, S., Mansell, D.J., Jervis, A., Lygidakis, A., Humphreys, L., Takano, E., Gardiner, J.M., and Scrutton, N.S. (2015). Enzymatic menthol production: one-pot approach using engineered *Escherichia coli*. ACS Synth. Biol. *4* (10), 1112–1123, https://doi.org/10.1021/acssynbio.5b00092.

Vanholme, R., Demedts, B., Morreel, K., Ralph, J., and Boerjan, W. (2010). Lignin biosynthesis and structure. Plant Physiol. *153* (3), 895–905, https://doi.org/10.1104/pp.110.155119.

Wen, L., Jiang, Y., Yang, J., Zhao, Y., Tian, M., and Yang, B. (2017). Structure, bioactivity, and synthesis of methylated flavonoids. Ann. N. Y. Acad. Sci. *1398* (1), 120–129, https://doi.org/10.1111/nyas.13350.

Wickham, H. (2011). ggplot2. WIREs Comput. Stat. *3* (2), 180–185, https://doi.org/10.1002/wics.147.

Woodrow, K.A., and Swartz, J.R. (2007). A sequential expression system for high-throughput functional genomic analysis. Proteomics *7* (21), 3870–3879, https://doi.org/10.1002/pmic.200700471.

Yin, G., Garces, E.D., Yang, J., Zhang, J., Tran, C., Steiner, A.R., Roos, C., Bajad, S., Hudak, S., Penta, K., et al. (2012). Aglycosylated antibodies and antibody fragments produced in a scalable in vitro transcription-translation system. mAbs *4* (2), 217–225, https://doi.org/10.4161/mabs.4.2.19202.

Youngdae, Y., Park, Y., Yi, Y.S., Lee, Y., Jo, G., Park, J.C., Ahn, J.H., and Lim, Y. (2010). Characterization of an O-methyltransferase from *Streptomyces avermitilis* MA-4680. J. Microbiol. Biotechnol. *20* (9), 1359–1366, https://doi.org/10.4014/jmb.1005.05012.

Yu, G., Tsan, T., Lam, Y., Zhu, H., and Guan, Y. (2018). Two methods for mapping and visualizing associated data on phylogeny using ggtree. Mol. Biol. Evol. *3* (35), 3041–3043, https://doi.org/10.1093/molbev/msy194.

Zahid Khan, M., and Nawaz, W. (2016). The emerging roles of human trace amines and human trace amine-associated receptors (hTAARs) in central nervous system. Biomed. Pharmacother. *83*, 439–449, https://doi.org/10.1016/j.biopha.2016.07.002.

Zhu, F., Zhong, X., Hu, M., Lu, L., Deng, Z., and Liu, T. (2014). In vitro reconstitution of mevalonate pathway and targeted engineering of farnesene overproduction in *Escherichia coli*. Biotechnol. Bioeng. *111* (7), 1396–1405, https://doi.org/10.1002/bit.25198.

Zubieta, C., Kota, P., Ferrer, J., Dixon, R.a., and Noel, J.P. (2002). Structural basis for the modulation of lignin monomer methylation by caffeic acid/5-hydroxyferulic acid 3/5-*O*-methyltransferase. Plant Cell *14* (June), 1265–1277, https://doi.org/10.1105/tpc.001412.nylpropanoids.

STAR★METHODS

KEY RESOURCES TABLE

REAGENT or RESOURCE	SOURCE	IDENTIFIER
Bacterial and Virus Strains		
Bacterial strains generated by plasmid transformation are listed in Table S3	This study	NA
Chemicals, Peptides, and Recombinant Proteins		
OMTs heterologously expressed in this study are listed in Table 1.	This study	NA
S-(5′-adenosyl)-L-methionine p-toluene	Sigma-Aldrich	Cat No.: A2408
1,2 Dihydroxybenzene	Sigma-Aldrich	Cat No.: 135011
3-OH-4-MeOH cinnamic acid	Sigma-Aldrich	Cat No.: 103012
Caffeic acid	Sigma-Aldrich	Cat No.: C0625
p-coumaric acid	Sigma-Aldrich	Cat No.: C9008
Ferulic acid	Sigma-Aldrich	Cat No.: 128708
Quercetin	Sigma-Aldrich	Cat No.: Q4951
Critical Commercial Assays		
myTXTL® Sigma 70 Master Mix Kit	Arbor Bioscience (Biodiscovery, LLC; Ann Arbor, MI, USA)	Cat No.: 507096
myTXTL GamS Nuclease Inhibitor Protein	Arbor Bioscience (Biodiscovery, LLC; Ann Arbor, MI, USA)	Cat No.: 501096
TR-FRET Bridge-It® S-Adenosyl Methionine (SAM) Fluorescence Assay Kit	Mediomics LLC (St. Louis, Missouri, USA)	Cat No.: TRF 1-1-1004A
Deposited Data		
Analyzed data	This study	NA
Experimental Models: Organisms/Strains		
E.cloni® 10G (F- *mcrA* Δ(*mrr-hsd*RMS-*mcr*BC) *end*A1 *rec*A1 Φ80*dlac*ZΔM15 Δ*lac*X74 *ara*D139 Δ(*ara*,*leu*)7697*gal*U *gal*K *rps*L *nup*G λ- *ton*A)	Lucigen (Middleton, Wi, USA)	VWR Cat No.: 89,002-678
E. coli BL21 DE3 strain (F^- *ompT gal dcm lon hsdS*$_B$($r_B^-m_B^-$) λ(DE3 [*lacI lacUV5-T7p07 ind1 sam7 nin5*]) [*malB*$^+$]$_{K\text{-}12}$(λ^S))	Prather Lab strain collection	NA
E. coli K12 MG1655 DE3 (F^- λ^- *ilvG- rfb*-50 *rph*-1 (DE3))	(Nielsen et al., 2010), Prather Lab strain collection	NA
Oligonucleotides		
Primers for cloning of expression plasmids are shown in Table S2	This study	NA
Recombinant DNA		
Sequences of synthetic DNA constructs encoding OMTs are provided in Data S2	This study	NA
Plasmids used in this study are listed in Table S2	This study	NA
Software and Algorithms		
HMMsearch EBI webtool version 2.23.0	Potter et al. (2018)	https://www.ebi.ac.uk/Tools/hmmer/search/hmmsearch
EFI-EST webtool	Gerlt et al. (2015)	https://efi.igb.illinois.edu/efi-est/
Cytoscape 3.8.0	Shannon et al. (2003)	https://cytoscape.org/download.html
Codon optimization webtool	Integrated DNA Technologies (Coralville, IA, USA)	https://www.idtdna.com/pages/tools/codon-optimization-tool?returnurl=%2FCodonOpt

(*Continued on next page*)

Continued

REAGENT or RESOURCE	SOURCE	IDENTIFIER
mafft v7.310	Nakamura et al. (2018)	https://mafft.cbrc.jp/alignment/software/
FastTree v2.1.10	Price et al. (2010)	http://www.microbesonline.org/fasttree/
R package ggplot2	Wickham (2011)	https://ggplot2.tidyverse.org/
R package ggtree	Yu et al. (2018)	https://guangchuangyu.github.io/software/ggtree/
GraphPad Prism 8	GraphPad Software (San Diego, CA, USA)	https://www.graphpad.com/scientific-software/prism/

RESOURCE AVAILABILITY

Lead contact

Further information and requests for resources and reagents should be directed to and will be fulfilled by the Lead Contact, Kristala L.J. Prather (kljp@mit.edu).

Materials availability

All strains and plasmids generated in this study are available upon request from the Lead Contact Kristala L.J. Prather (kljp@mit.edu).

Data and code availability

The published article includes all datasets generated during this study. Raw data are available upon request from the Lead Contact.

EXPERIMENTAL MODEL AND SUBJECT DETAILS

Molecular cloning, protein expression and fermentation experiments were performed in *Escherichia coli*.

All molecular cloning and plasmid propagation steps were performed in the chemically competent strain *E. cloni* 10G (F- *mcrA* Δ(*mrr-hsd*RMS-*mcr*BC) *end*A1 *rec*A1 Φ80*dlac*ZΔM15 Δ*lac*X74 *ara*D139 Δ(*ara*,*leu*)7697*gal*U *gal*K *rps*L *nup*G λ-*ton*A) produced by Lucigen (Middleton, WI, USA). The cultures were maintained at 30°C in Luria Bertani (LB) medium with the respective antibiotics.

Protein expression was performed in the chemically competent *E. coli* BL21 DE3 strain (F^- *ompT gal dcm lon hsdS*$_B$($r_B^-m_B^-$) λ(DE3 [*lacI lacUV5-T7p07 ind1 sam7 nin5*]) [*malB*$^+$]$_{K\text{-}12}$(λ^S)). The strain was maintained at 37°C in selective LB medium containing 100 μg/mL carbenicillin. After induction of protein expression, the temperature was shifted to 30°C.

Fermentation for ferulic acid production was performed in the chemically competent *E. coli* K12 MG1655 DE3 strain transformed with three plasmids (Nielsen et al., 2010). The strain was maintained in selective LB medium at 37°C until induction of enzyme expression, when the medium was exchanged for selective modified M9 minimal medium and the temperature was shifted to 26°C. M9 medium composition (1x) prepared from sterile stocks: M9 salts (Millipore-Sigma, used as 5x stock), Trace Mineral Supplement (ATCC MD-TMS, used as 200x stock), vitamin mix (from 100x stock; final: riboflavin 0.84 mg/L, folic acid 0.084 mg/L, nicotinic acid 12.2 mg/L, pyridoxine 2.8 mg/L, and pantothenic acid 10.8 mg/L), biotin (from 1000x stock; final: 0.24 mg/L), thiamine (from 1470x stock; final: 340 mg/L), δ-Aminolevulinic acid (from 1000x stock in MeOH, final: 7.5 μg/mL), IPTG (from 1000x stock, final: 1 mM), carbenicillin (from 1000x stock, final: 100 μg/mL), spectinomycin (from 1000x stock, final: 50 μg/mL), kanamycin (from 1000x stock, final: 50 μg/mL, 4% (w/v) glucose (from 50% w/v stock). Additives for media optimization experiments: caffeic acid (from fresh 100x stock in MeOH, final 2 mM) and either a) no further additives, b) $MgCl_2$ (from 500x sterile stock in water, final 2 mM) or c) $MgCl_2$ (from 500x sterile stock in water, final 2 mM) and L-methionine (from fresh 100x stock in 1M HCl, final 10 mM). Additives for all other experiments: $MgCl_2$ (from 500x sterile stock in water, final 2 mM) and L-methionine and L-tyrosine (from fresh joined 100x stock in 1M HCl, final 10 mM and 3 mM, respectively).

All genes expressed in the myTXTL lysate are listed in Table 1. All plasmids used for enzyme expression and fermentation experiments are listed in Tables S2 and S3.

METHOD DETAILS

Selection of enzymes of interest

Two different multiple sequence alignments of known OMTs were generated with the Clustal Omega EBI webtool (Sievers et al., 2011) (Table S1) and used as input for HMMsearch (EBI webtool version 2.23.0 (Potter et al., 2018); database of reference proteomes of all taxa excluding green plants (taxid: 33,090), significance E-value cut-off 0.01 for the entire sequence and 0.03 for hits). The significant results were combined into one dataset (Document S1) and used as an input for calculating a sequence similarity network with a webtool of the Enzyme Function Initiative (EFI-EST (Gerlt et al., 2015); node selection cut-off: protein length between 180 and 400 amino acids, edge selection cut-off: alignment score >30). The finalized network was visualized in Cytoscape 3.8.0 (Shannon et al., 2003) with the yFiles organic layout. For the representation in Figure S4, the nodes were further filtered to exclude all nodes with

an HMM score below 70 and all edges with sequence identity below 50%. From the thus generated clusters enzymes were chosen for experimental characterization (Table 1).

Design and synthesis of DNA templates for TXTL reactions

The selected genes were codon-optimized for expression in *E. coli* with the Integrated DNA Technologies (IDT) optimization algorithm and manually modified to exclude recognition sites for BsaI, NcoI, XhoI and where possible NdeI restriction enzymes. The 5′ end of all DNA fragments was designed with an overhang of 500bp, the p70a promoter sequence and an NcoI recognition site to facilitate cloning into the pET21b(+) (Novagen) and pBEST (Arbor Bioscience) expression vectors. The 3′ end was designed to include an XhoI recognition site, the T500 terminator and a 500bp overhang. The synthetic DNA was obtained from Arbor Bioscience (Ann Arbor, MI, USA) with an additional purification step to allow for direct use in the myTXTL reaction for linear templates. The sequences of all synthetic DNA constructs is provided in Data S2.

Construction of plasmids

Genes encoding for OMTs selected for *in vivo* testing were cloned directly from the synthetic DNA fragments by restriction and ligation (NcoI/XhoI) into pET21b(+) for expression under the T7 promoter (Table S2). From there the genes were amplified by polymerase chain reaction (PCR) with gene specific 5′primers and the T7 terminator primer to generate an NdeI recognition site at the 5′ prime end. The PCR products were inserted by restriction and ligation (NdeI/XhoI) into the second multiple cloning site of the plasmid c71 (pRSF:FjTAL) for expression under the T7 promoter (Table S2). All constructs were verified by sequencing by ETON Bioscience (Charlestown, MA, USA). Plasmids c71, c84 and c86 were constructed in a previous study (Haslinger and Prather, 2020).

In vitro transcription/translation

In vitro transcription/translation was performed with the myTXTL kit from Arbor Bioscience according to the manufacturer's instructions. In brief, the synthesized DNA fragments were dissolved in nuclease-free water to a final concentration of 109.1 nM and stored at −70°C between experiments. All assay components were thawed on ice (myTXTL lysate, GamS protein and DNA templates) and mixed by carefully pipetting up and down. To minimize pipetting errors, a master mix of myTXTL lysate (9μL per reaction) and GamS protein (0.8 μL per reaction) was prepared on ice and aliquoted into 1.5 mL microcentrifuge tubes. 2.2 μL of DNA template were added to each tube and mixed by carefully pipetting up and down (final concentration 20 nM). The reactions were incubated on ice for 5 min and then transferred to a water bath at 29°C for 16 hr. As negative controls ("no OMT"), one reaction was performed with a DNA template not encoding for an OMT enzyme but the *Corynebacterium glutamicum* transcription factor mcbR, and one reaction with nuclease-free water without DNA.

SDS PAGE

To visualize protein expression 1 μL of the TXTL reactions was mixed with 2 μL of water and 3 μL of 2x Laemmli loading dye (Bio-Rad, Hercules, CA, USA) and incubated at 90°C for 3 min. The denatured samples were loaded onto AnyKD Mini-PROTEAN TGX precast protein gels (Bio-Rad, Hercules, CA, USA) and separated for 40 min at 40 mA. Protein bands were visualized by staining with InstantBlue protein stain and imaging with the Bio-Rad ChemiDoc imager.

Expression and purification of MxSafC

Plasmid c157 was transformed into chemically competent *E. coli* BL21 DE3 and maintained on selective LB agar containing 100 μg/mL carbenicillin. A starter culture was inoculated from a single colony (5 mL, LB with carbenicillin) and incubated overnight at 37°C, 250 rpm. The main culture was inoculated from the starter culture (1:100) and incubated at 37°C, 250 rpm until an optical density OD_{600} of 0.7 was reached. Expression was induced with Isopropyl β-D-1-thiogalactopyranoside (IPTG, 1 mM final) and the temperature was lowered to 30°C (250 rpm, overnight). All following steps were performed at 4°C with chilled buffers. The cells were harvested by centrifugation (10 min, 3,000 rpm) and resuspended in 20 mL lysis buffer (buffer A including one EDTA-free protease inhibitor tablet (Roche) and 10 mg/mL lysozyme; buffer A: 50 mM Tris/HCl pH 7.4, 500 mM NaCl, 10 mM imidazole). The cell suspension was incubated on ice for 20 min, lysed by sonication (20% duty cycle, 10 cycles of 15 s ON/15 s OFF) and cleared by centrifugation for 20 min at 40,000 x g. The supernatant was loaded onto the affinity matrix equilibrated with buffer A by gravity flow (Qiagen, Ni-NTA agarose slurry, 0.25 mL column volume). The column was washed with 20 column volumes of buffer A and eluted stepwise with one column volume of buffers B1 to B6 (buffers B1-B6: 50 mM Tris/HCl pH 7.4, 500 mM NaCl, 50 mM imidazole/100 mM imidazole/150 mM imidazole/200 mM imidazole/250 mM imidazole or 500 mM imidazole, respectively). The eluates of each step were collected in separate fractions and analyzed by SDS PAGE. MxSafC containing fractions with low protein background were pooled and dialyzed overnight at 4°C against storage buffer (20 mM Tris/HCl pH 7.4, 50 mM NaCl, 0.2 mM $MgCl_2$, 2 mM DTT). The protein concentration was determined by absorbance at 280 nm (NanoDrop, ThermoFisher Scientific, USA) before the purified enzyme was aliquoted and stored at −70°C.

In vitro OMT reaction

The *in vitro* OMT reaction was adapted from the conditions used by Siegrist et al.(Siegrist et al., 2017). To minimize pipetting errors, a master mix including all reaction components, but the enzyme was prepared (50 mM HEPES/NaOH pH 7, 20 mM $MgCl_2$, 2 mM SAM, 2 mM substrate (from 40x stock in DMSO)). The total reaction volume was 42 μL, with 5 μL of diluted TXTL reaction (2.5-fold dilution in OMT reaction buffer) to further minimize pipetting errors. After aliquoting the master mix into 96-well microtiter plates (200 μL

round-bottom plates), the TXTL samples were added and mixed by carefully pipetting up and down. Purified MxSafC enzyme (0.84 mg/mL stock) was included in one well as a positive control. The "no OMT" controls (see section "*In vitro* transcription/translation") were treated like the other enzyme samples. The sealed plates were incubated at 30°C for 24 hr before the reactions were quenched with $HClO_4$ (final 2% v/v from a 10% v/v stock) and centrifuged. The supernatants were analyzed by Time Resolved-Fluorescence Energy Resonance Transfer (TR-FRET) and (optionally) by High-Performance Liquid Chromatography (HPLC).

TR-FRET assay for SAM detection

To detect the consumption of the SAM co-factor as a measure of OMT reactivity, we used the TR-FRET Bridge-It S-Adenosyl Methionine (SAM) Fluorescence Assay Kit from Mediomics LLC (St. Louis, Missouri) according to the manufacturer's instructions with slight modifications. In brief, we thawed the assay solution at 37°C for 30 min and transferred 18 μL into the wells of a white 384-well round-bottom polystyrene plate (Corning, NY, USA). We diluted the quenched OMT reactions 21-fold by mixing 2 μL of the reaction with 40 μL of water by pipetting up and down, and transferred the samples to the 384-well plate without bubbling. In addition to the "no OMT" controls (no SAM consumption expected), one or two wells were measured with only the TR-FRET assay solution (20 μL, "blank"). The plate was incubated in the dark for 30 min at room temperature before measuring the TR-FRET signal in a Tecan Infinite-200 plate reader with the following settings: *mode*: fluorescence top reading, *excitation wavelength*: 340 nm, *emission wavelength*: 667 nm, *excitation bandwidth*: 9 nm, *emission bandwidth*: 20 nm, *gain*: 220 (manual), *number of flashes*: 100, *integration time*: 400 μs, *lag time*: 50 μs, *settle time*: 150 ms. The ratio of the acceptor channel counts to the donor channel counts was calculated for all measured wells (FRET), baseline corrected with the FRET ratio of the "blank" and normalized to the average of the FRET ratio of the "no OMT" controls. This value is plotted in the y axis of the respective figures labeled as "substrate ratio: [sample/neg. control]". In the initial experiment, the samples were handled with single-channel pipettes, whereas in the later experiments, multichannel pipettes were used throughout to minimize pipetting errors.

$$y = \frac{(FRET_{sample} - FRET_{blank})}{Average(FRET_{noOMT} - FRET_{blank})}, \text{ with } FRET = \frac{counts_{667nm}}{counts_{620nm}}$$

Fermentation

The OMT encoding plasmids were transformed into chemically competent (Inoue et al., 1990) *E. coli* K12 MG1655(DE3) (Nielsen et al., 2010) already bearing the plasmids c84 and c86 encoding for CYP199A2 F185L NΔ7 and its redox partners putidaredoxin (Pux) and putidaredoxin reductase (PuR). All strains generated in this way are listed in Table S3. The final strains were maintained on selective media with carbenicillin, spectinomycin and kanamycin at all times. Starter cultures were prepared from three individual colonies of the final strains in 5 mL Lysogeny broth (LB) supplemented with carbenicillin (100 μg/mL), spectinomycin (50 μg/mL) and kanamycin (50 μg/mL) in round-bottom polystyrene tubes, incubated over night at 37°C with agitation and used to inoculate the main cultures (7 mL LB with antibiotics; round-bottom polystyrene tubes). After 4 hr of growth at 37°C, 250 rpm, OD_{600} was measured and the appropriate volume of each culture pelleted and resuspended in modified, selective M9 medium including substrates and 4% glucose to obtain 15 mL cultures at OD_{600} of 0.7 in sterile glass tubes. These cultures were incubated at 26°C, 160 rpm for 96 hr. Samples of 200 μL were taken after 96 hr and quenched with 50 μL of $HClO_4$ (10% (v/v) stock), spun for 10 min at 20,000 x g and the supernatants were analyzed by HPLC. Media optimization was performed in small scale (5 mL in round-bottom polystyrene tubes) throughout the entire experiment.

HLPC analysis

The supernatants of the quenched *in vitro* OMT reactions and fermentation samples were analyzed by reversed-phase HPLC (instrument: Agilent 1100; autosampler: HiP sampler G1367A, T = 4°C, 10 μL injection; column: Agilent Zorbax Eclipse XDB-C18 80Å, 4.6 × 150 mm, 5μm, T = 30°C; detector: Agilent diode array detector G1315B, λ = 275 nm (catechol and methylated products) and λ = 310nm ((iso-)ferulic acid and pathway intermediates); gradient: 10%–35% Acetonitrile with 0.1% Trifluoracetic acid over 17 min). The peaks for products and intermediates were identified by comparing the retention times to authentic standards. The integrated peak areas were converted to concentrations in mM based on calibration curves generated with authentic standards (see Figure S2). For separation of SAM and SAH as shown in Figure S2C and S2D, the samples were analyzed with a Shimadzu LC-10 AT pump and SPD-M10A diode array detector. Column, solvent gradient and run conditions were identical to the separations with the Agilent HPLC.

Sequence analysis of putative OMTs

We aligned the sequences with mafft v7.310 (Nakamura et al., 2018) b (–genafpair), inferred the maximum likelihood phylogenies with FastTree v2.1.10 (Price et al., 2010) and visualized the tree and the corresponding activity heatmap in Figure 4 with the R packages ggplot2 (Wickham, 2011) and ggtree (Yu et al., 2018).

QUANTIFICATION AND STATISTICAL ANALYSIS

No statistical analysis was performed. The sample size, the definition of replicates and error bars is provided in the figure captions.